# PERIODIC TWO-PHASE HEAT TRANSFER COEFFICIENTS IN AN ELECTRONIC COOLING MINI EVAPORATOR

**S. Filippeschi, E. Latrofa, G. Salvadori**
Department of Energetic "Lorenzo Poggi" Pisa University
Via Diotisalvi, 2 – 56100 – Pisa – Italy
Tel: +39/050/569634 Fax: +39/050/569666
s.filippeschi@ing.unipi.it, e.latrofa@ing.unipi.it, g.salva@ing.unipi.it

**Abstract**

In the case of indirect cooling, the metallic mass of the evaporator can play an important role in all periodic cooling devices. This paper presents two different methods of measuring an heat transfer coefficient changing over time. The first method determines the output power removed by the fluid by measuring the temperature close to the heat transfer surface and approximating the temperature distribution in the copper evaporator with a finite difference method, while the second method directly measures the two-dimensional temperature distribution in the evaporator. Both methods have shown good accordance if applied to a PTPT device with a periodic heat transfer coefficient. The PTPT device presents a maximum heat transfer coefficient of 11000 $W/m^2 \cdot K$ if the periodic liquid pool volume in the evaporator is higher than $64 \cdot 10^{-6}$ $m^3$, while it falls to 5000 $W/m^2 \cdot K$ if the periodic liquid pool volume in the evaporator is lower than $3.5 \cdot 10^{-6}$ $m^3$. This evaporator, with a mass of 0.155 kg, presents temperature oscillations lower than 6 K even in the case of a liquid pool volume of $3.5 \cdot 10^{-6}$ $m^3$.

**KEYWORDS**

Transient boiling coefficient, miniature evaporator, Periodic Two Phase Thermosyphon (PTPT), electronic cooling.

## INTRODUCTION

The quick growth in the use of electronic packaging has created critical values for maximum heat flux dissipation. Nowadays heat pipes, LHPs and CPLs are really the most efficient cooling systems, but their high costs can limit their use in commercial devices. Recent innovations in wickless devices have had a growing impact on the electronic equipment thermal control for high density desktop computers. The most commonly implemented devices are the two-phase loop thermosyphons, which can be used either for direct or indirect cooling. In 1997 McDonald et al. [1] studied the performance characteristics of a loop thermosyphon. In 1998 Ramaswamy and Joshi [2] designed a loop thermosyphon with a copper microstructure dissipator which gave a better performance than in one with a plain surface. This evaporator could dissipate more than $10 \cdot 10^5$ $W/m^2$ with a wall superheat of 27.5 K by using FC72 as working fluid. Besides, these authors found that the effect of the inclination and the liquid fill volume on the heat transfer coefficient was marginal. In 1999, Na et al. [3] applied a two-phase loop thermosyphon to the MCM module cooling, with R11 as working fluid and micro fins in the cold plate evaporator. In 1999 Rhi and Lee [4] experimented a loop thermosyphon for electronic cooling by using several working fluids (acetone, R11, water, FC 72, FC87, ethanol and R113). The evaporator dimensions were 50x50x8 $mm^3$ and the best performance achieved was $12 \cdot 10^4$ $W/m^2$, with a wall superheat of 50 K and using Ethanol or FC 87 as working fluid. On the other hand a maximum heat flux of only $10 \cdot 10^4$ $W \cdot m^{-2}$ was reached with FC72.

In 2001 Yuan et al. [5] looked into the evaporator and condenser location-specific design issues for the thermosyphon. In 2002 Krustalev [6] presented a U tube flat evaporator for electronic cooling in a miniature loop thermosyphon with the condenser placed 0.6 m over the evaporator. A maximum heat flux of $70 \cdot 10^4$ $W/m^2$ was reached with methanol as working fluid and a capillary structure on the cooled surface of the evaporator. In 2002 Patel and Joshi [7] presented a compact two-phase loop thermosyphon with a copper evaporator of 32x32x29 $mm^3$, with a particular enhanced surface inside. They noted good performances for all the tilt angles within the range –58° ÷ +36°, with PF5060 (boiling temperature 56°C) or water as working fluids.

However, one of the most important cooling limits of a pool boiling thermosyphon is the CHF. Given the stringent volume constraints of electronic cooling hardware, only a small mass of dielectric

liquid can be permitted, and the small confines of the liquid pool could limit greatly the CHF. For this reason much research activity on mini and micro channel evaporators has been carried out, but a liquid or two-phase flow which must be forced through them creates wide pressure drops. Miniature two-phase loop thermosyphons could not, therefore, have sufficient head loads to allow working fluid circulation, while micro and mini active pumps have high costs and low reliability.

In 2003 Mudawar and Mukherjee [8] presented two types of evaporator electronic cooling inserted in a loop thermosyphon with flat and micro-channel surfaces. By placing the surface vertically and reducing the gap separating it from the flat wall opposite, they observed a CHF enhancement both with flat and micro-channel surfaces. In particular, with FC72 as working fluid they observed CHF values 4.5 and 5.9 times greater than those for pool boiling in the case of a flat and a micro-channel evaporator, respectively. In 2005 Khodabandeh [9] presented a loop thermosyphon for the cooling of a radio base station. In this case the evaporator sizes were 9.53x9.53x95 $mm^3$ and the difference between evaporator and condenser was 1.29 m. The thermosyphon could remove a heat flux of up to $10 \cdot 10^5$ $W/m^2$ with Isobutane as fluid.

The studies just mentioned show the prospects for two-phase loop thermosyphons in compact devices, for electronic cooling. However, these devices do not allow great flexibility in the location of the remote condenser with respect to the evaporator, and this topic could be severely limit their use.

In the literature there is a particular kind of two-phase loop thermosyphon which is able to operate with the condenser located anywhere with respect to the evaporator, without an increase in thermal resistance [10]. These devices, which operate in a periodic heat transport regime, are called Periodic Two-Phase Thermosyphons (PTPT).

The present authors have recently studied the possibility of applying a PTPT device to microelectronic cooling with good results [11]. In particular, a stable periodic regime has been reached even with only $3.5 \cdot 10^{-6}$ $m^3$ of working fluid periodically circulating in the evaporator for heat fluxes close to the CHF for plain surfaces. In previous experiments a maximum heat flux of $16 \cdot 10^4$ $W/m^2$ was dissipated from a plain surface with FC72 as working fluid [12].

In a PTPT the evaporator operates with a variable pool of liquid, which may be even equal to zero for a few seconds. The heat transfer coefficient inside the evaporator therefore varies periodically every cycle. For instance, it can vary over 200 seconds from typical values for boiling heat transfer conditions (about 7000-10000 $W/m^2$) down to about 400-500 $W \cdot m^{-2}$. In these conditions the thermal capacity of the miniature evaporator becomes important in reducing the temperature oscillations on the cooled chip. This paper describes how the heat transfer coefficient can be experimentally measured over set intervals in a mini evaporator working in a PTPT device.

## EXPERIMENTAL FACILITY

The tested PTPT loop consists of 3 main components: evaporator (internal volume $238 \cdot 10^{-6}$ $m^3$), condenser ($10 \cdot 10^{-6}$ $m^3$) and accumulator ($70 \cdot 10^{-6}$ $m^3$). They are connected in a loop with different connections ($34 \cdot 10^{-6}$ $m^3$) as shown in Fig. 1. The condenser, air-cooled by a fan, is made of a 64x78x8 $mm^3$ aluminium plate, with 22 rectangular fins 28 mm high, 78 mm long and 1.3 mm thick. Inside the plate a serpentine groove has been manufactured covering a 4x4 $mm^2$ section surface. All the connections are flexible polyethylene pipes with an internal diameter of 4 mm. The stainless steel solenoid valves are of 2-way type, normally closed with an opening response time of 5 ms.

The electronic component is simulated by a copper dissipator heated by a thermo-heater. The mass of the copper dissipator is 0.123 kg. The surface wetted by the working fluid is $2.77 \cdot 10^{-4}$ $m^2$. A ring, made of PTFE, thermally disconnects the copper dissipator from the aluminium case of the evaporator. The low surface of the copper dissipator is not thermally insulated ($D_e$=0.038m, $\Delta z$=0.01 m, Fig. 3) and it is surrounded by air at a temperature of 297±2 K. The working fluid is FC72.

The control system consists of a digital timer (0.01 s to 1000 hours), covering various operational modes. In the experiments it is set with a period when the valves are off ($\Delta t_1$) and a period when the valves are on ($\Delta t_2$). The temperature of the plain surface $T_w$ is measured by a K-type thermocouple 0.5 mm thick. It is located 2 mm under the surface of the copper dissipator. All the thermocouples are of K-type, 1 mm thick, and measure the following temperatures: temperature of liquid pool $T_{ev,l}$ placed 1 mm above surface and the saturation temperature of the vapour $T_{ev,v}$ inside the evaporator.

The lower part of the copper dissipator is covered with a film of known emittance ($\varepsilon$ = 0.99) which makes it possible to measure its two-dimensional temperature distribution with an infrared thermo-camera. The infrared thermo-camera has a Focal Plane Array of two-dimensional micro-bolometric sensors, with a digital resolution of 320x240. It is sensitive to radiations with wave lengths of 8÷14

μm, which allows a reduction of the thermal noise due to the environmental air conditions. The minimum thermal resolution is 0.15 K. The optical system consists of a 35 mm lens, with a field of view of 25.8° x 19.5° and an instant field of view of 1.4 μrad. The minimum distance necessary to bring the image into focus is 0.3 m. The infrared system captures a frame every 0.03 s.

The vapour pressure inside the accumulator and evaporator are measured by a Druck PTX 75-11 transmitter (0÷2.5 bar, accuracy 0.25% of full scale range). The volume $V_T$ of working fluid transferred in every cycle has been measured by a level meter located inside the accumulator: its accuracy is about $\pm 0.76 \cdot 10^{-6}$ m$^3$. All the temperatures and pressures within the device are sampled by an Agilent 34970A data acquisition system (thermal resolution 0.1 K, accuracy ±0.5 K, minimum acquisition frequency 3 Hz) and stored in a PC microcomputer. The tests have been carried out by starting from the same volume ($160 \cdot 10^{-6}$ m$^3$) and temperature of liquid in the loop, but changing the volume $V_T$ which periodically circulates in the evaporator. For each volume $V_T$, different input powers supplied to the evaporator $\dot{Q}_e$ have been tested.

## PERIODIC HEAT TRANSFER COEFFICIENT

The PTPT device operates in a stable periodic regime. The operating modes of a PTPT are described in [13], [14], but, once a stable regime has been reached, for each cycle pressure, wall superheat and volume of liquid inside the evaporator change over time. In particular, the volume of liquid at the starting and ending time of a single cycle $V_{e,l}(t_0)$ and $V_{e,l}(t_2)$ is exactly equal to $V_T$, but there is a time $t_1$ when it falls to zero. During a single cycle, therefore, different heat transfer regimes can be expected. Some qualitative considerations on the heat transfer regime experimentally observed over time have been made in [12] with reference to evolutions in temperatures $T_W$ and $T_S$ and their differences $(T_W\text{-}T_S)$, which are shown in Fig. 2. The data in Fig. 2 are relative to $\dot{Q}_e$=30 W ($q_d$=$14.44 \cdot 10^4$ W/m$^2$ ) and a transferred volume $V_T$ of working fluid of about $25 \cdot 10^{-6}$ m$^3$.

The wall superheat evolution in a single cycle has been divided into 6 parts (I-VI, Fig. 2). Part I (0-10 s) is characterised by a fall in wall superheat: the temperature $T_W$ decreases, while $T_S$ increases. In part I all the volume $V_T$ is inside the evaporator. Part II (10-60 s) is different from part I because $T_S$ stays constant. In these parts the copper dissipator gives the heat previously stored $\dot{Q}_a$ to the fluid, and the volume of liquid pool $V_{e,l}$ decreases in time. In part III (60-120 s) the wall superheat remains unchanged, while the volume of liquid pool $V_{e,l}$ continues to decrease. In part IV (120-230 s) the volume $V_{e,l}$, reaches zero and the copper dissipator surface is now in contact with the vapour.

Part IV is characterised by a transition heat transfer regime between the nucleate boiling regime of part III and the convective heat transfer of part V (230-240 s). This effect on the heat transfer coefficient depends on the fluid-dynamic field of the liquid pool and it can, therefore, depend on the geometrical effect (shape of the evaporator), location of the return tube in the pool and volume of the pool. A steady state analysis of each single effect on the boiling heat transfer and CHF is currently being studied by the present authors. Lastly, in part VI (240-265 s) the return of the cold liquid on the dissipator surface occurs. Part VI starts with the opening of the valves and finishes with their closing.

These experimental results show that the heat transfer coefficient changes greatly over time in a PTPT device. The heat transfer regimes experimentally observed are different in time: liquid convective, transition boiling, boiling and vapour convection. The heat transfer coefficient periodic function in time is similar in shape for different $V_T$, but changes greatly in its maximum value. The temperature oscillations induced by the changes in the heat transfer coefficient are, therefore, influenced by this function. The thermal capacity of the copper dissipator can play an important role as dumper of the temperature oscillations in the chip. For this reason it is important to measure the different heat transfer coefficient functions in time in a PTPT device at different liquid pool volumes transferred every cycle, once a stable periodic regime has been reached.

### Preliminary analysis

The transient heat transfer coefficient $h(t)$ in the evaporator is expressed by eq.(1)

$$h(t) = \frac{\dot{Q}_d(t)}{S_d \cdot \left[T_W(t) - T_S(t)\right]}, \tag{1}$$

where $S_d$ ($\pi D_d^2/4$) is the heat transfer surface of the dissipator wetted by the liquid, $\dot{Q}_d(t)$ is the power dissipated from the surface $S_d$, and $T_W(t)$ and $T_S(t)$ are the temperatures of the copper dissipator wall and the saturated vapour, respectively. The temperatures $T_W$ and $T_S$ are measured over time (time increments 3 s, locations A e B, Fig.1), but the only power directly measured over time is $\dot{Q}_e$. The power $\dot{Q}_d(t)$ can be determined, at a generic time t, by the following thermal power balance:

$$\dot{Q}_e(t) = \dot{Q}_d(t) - \dot{Q}_a(t) - \dot{Q}_{env}(t), \tag{2}$$

where $\dot{Q}_a$(t) is the heat stored by the dissipator for each time increment and $\dot{Q}_{env}$(t) is the power loss. If the power loss through the PTFE ring is considered negligible, $\dot{Q}_{env}$(t) is equal to the power dissipated in the environment by the lower part of the copper dissipator. An initial evaluation of this power can be made by using the experimental data reported in [12] and the Squire-Eckert correlation [15], modified in the case of vertical cylinders [16], for the free convective heat transfer evaluation. The maximum heat transfer calculated is below 11.5 W/m$^2$ K and the maximum thermal power $\dot{Q}_{env}$ is below 3% of $\dot{Q}_e$: it has, therefore, been neglected in this paper.

In conclusion, in order to calculate the power $\dot{Q}_d$ in time by eq.(2), an accurate evaluation of $\dot{Q}_a(t)$ is necessary. However, this paper proposes two methods for $\dot{Q}_d(t)$ measurement, the first (Method A) by eq.(2) with the evaluation of $\dot{Q}_a(t)$, the second (Method B) by measuring the thermal gradient in the copper dissipator with an infrared thermo-camera. The Method B can be used with low errors, only under the particular hypothesis described below.

**Measurement Method A**

The $\dot{Q}_a(t)$ evaluation can be made if the copper dissipator's three-dimensional temperature distribution in time is known, but the problem can be reduced to a two-dimensional case, because the copper dissipator presents an axial-cylindrical symmetry (independence of angular coordinate $\theta$).

In order to approximate the function $T(r,z,t)$ in the copper dissipator, a transient finite difference method has been used. The copper dissipator has, therefore, been divided into 10 nodes, as shown in Fig. 3, with a variety of control volumes $V_i$ (diameter $D_i$ and length $L_i$, $1 \le i \le 10$). The control volume of each node has been chosen in order to obtain a Biot number lower than 0.1, with a heat transfer coefficient equal to $11 \cdot 10^3$ W·m$^{-2}$·K$^{-1}$ : this heat transfer coefficient is relative to the boiling regime between a plain surface and the FC72 [17] [18]. The time increment used in the time approximation is equal to the time between two measurements (3 s).

Performing an energy balance on a control volume for each generic surface node $i$, the implicit form of the finite difference equation, for the time step n, is eq.(3)

$$\frac{T_{i-1}^{n+1} - T_i^{n+1}}{R_{i-1,i}} - \frac{T_i^{n+1} - T_{i+1}^{n+1}}{R_{i,i+1}} = M_i \cdot c \cdot (T_i^{n+1} - T_i^n) / \Delta t, \tag{3}$$

where $R_{i-1,i}$ is the conductive thermal resistance between nodes $i$ and $i-1$, $M_i$ is the mass of node $i$ and $c$=385 J/(Kg K) is the copper specific heat.

The energy balances of the boundary nodes 1 and 10 are expressed by the following equations:

$$\dot{Q}_e - \frac{T_1^{n+1} - T_2^{n+1}}{R_{1,2}} = M_1 \cdot c \cdot (T_1^{n+1} - T_1^n) / \Delta t; \tag{4}$$

$$\frac{T_9^{n+1} - T_{10}^{n+1}}{R_{9,10}} - h^{n+1} \cdot S_d \cdot (T_W^{n+1} - T_S^{n+1}) = M_{10} \cdot c \cdot (T_W^{n+1} - T_W^n) / \Delta t, \tag{5}$$

where $T_W^{n+1}$ and $T_S^{n+1}$ are the temperatures experimentally measured at time $t=(n+1)\cdot\Delta t$. The energy balance written for every node creates a linear system of 10 equations with 9 unknown temperatures

($T^{n+1}$ in the nodes 1-9) and 1 unknown heat transfer coefficient $h^{n+1}$. The starting conditions of the system are $T_i^0 = \dot{Q}_e \cdot R_{i,i+1} + T_{i+1}^0 \quad 1 \le i \le 9; \quad h^0 = \dot{Q}_e /(S_d \cdot (T_{10}^0 - T_{sat}^0))$.

The main results of this analysis are shown in Fig. 4-6. Fig. 5 and Fig. 6 show the evolutions of the heat transfer coefficient *h*, in the case of different values of $V_T$, for $\dot{Q}_e$ =30 and 40 W, respectively.

The heat transfer coefficient function assumes a shape similar to a square wave. At the start and at the end of the cycle, in fact, a sudden rise and fall have been observed. These rapid changes are observed with the open valves and the fall of *h* is slower than its rise. The increase in *h* is determined by the thermal release of the stored heat $\dot{Q}_a$, but the fall can be determined only by a decay in heat transfer. In this part, as the liquid pool shrinks, the fluid-dynamic inside the liquid in the evaporator influences the heat transfer coefficient. The minimum heat transfer coefficient experimentally measured is in the range 1000-2000 W/m$^2$·K for different $V_T$ and $\dot{Q}_e$. This heat transfer coefficient is measured as the liquid leaves the evaporator. In this time (10-12 s) the heat transfer coefficient shows an oscillation of 3000-4000 W/m$^2$·K. Unfortunately, this method allows only 3-4 measurements to be made in this time and its accuracy is poor.

Lastly, the heat transfer coefficient function *h(t)* depends on the volume $V_T$. For high $V_T$ (>65·10$^{-6}$ m$^3$) in the middle part of the single periodic cycle (50<t<200 s, Fig. 5), a heat transfer similar to a pool boiling regime is observed and *h(t)* is approximately constant [12]. This is the maximum heat transfer coefficient measured in this device. In other cases [12], the heat transfer coefficient *h(t)* decreases with $V_T$, down to 5000 W/m$^2$·K if $V_T$ =3.5·10$^{-6}$ m$^3$ (Fig. 5). Fig. 6 shows the evolutions of the power $\dot{Q}_e$, $\dot{Q}_d$ and $\dot{Q}_a$ in a single stable periodic regime. The experimental data are relative to a $V_T$ =25·10$^{-6}$ m$^3$ and $\dot{Q}_e$ =30 W. The quantity $\dot{Q}_a$, at the generic time increment *n*, has been calculated by taking into account the difference of temperature $(T_i^{n+1} - T_i^n)$ for each node, while $\dot{Q}_d$ has been indirectly determined by eq.(2). Fig. 6 shows that $\dot{Q}_a$ presents a sudden increase a few seconds before the opening of the valves, with the evaporator dry. At this time $\dot{Q}_a$ is 33% of $\dot{Q}_e$. This question can play an important role in reducing the dimensions of the metallic evaporator, because small evaporator mass could induce high temperature oscillations on the cooled chip. Moreover, Fig. 7 shows the evolution of the temperature of every node for a single heat transfer cycle. The maximum amplitude of the oscillation of temperature falls with the distance from the surface wetted by the liquid. But it falls 1 K in 10 mm, and this effect is not relevant in the choice of the shape of the evaporator. This evaporator, with a mass of 0.155 kg, presents temperature oscillations lower than 6 K even in case of $V_T$ =3.5·10$^{-6}$ m$^3$, but if a copper mini evaporator with a mass of 0.062 kg is taken into account, the oscillation temperatures are, however, lower than 15 K.

**Measurement Method B**

The method B allows the evaluation of $\dot{Q}_d(t)$ by the measurement of a two-dimensional temperature map in a low part of the copper dissipator by a infrared thermo-camera. Fig. 8 shows three different infrared images of the evaporator at different times if $\dot{Q}_e$=30 W and $V_T$ =25·10$^{-6}$ m$^3$.

The thermo-camera allows *T(r,z)* every 0.03 s to be measured in the portion of the copper dissipator that has no thermal insulation. The surface observed is semi-cylindrical, with a diameter of 0.038 m and a height of 0.01 m, while the image of the copper dissipator is a rectangular area divided into 1575 pixels of 6·10$^{-5}$x6·10$^{-5}$ m. In this way 25 pixels are in direction *z* and 63 pixels in direction *x* (where $x = r \cdot \cos(\theta)$).

The first problem connected with the accuracy of the measurement derives from the variations in the factor of view between different areas – identified by a single pixel on the semi-cylindrical surface – and the thermographic instrument. The factor of view influences the heat radiating flux emitted by the each pixel and, therefore, influences the temperature measured by the instrument. From experimental analysis it can be seen that a solid angle lower than 60° does not influence the temperature measured, taking into account the spatial resolution of the instrument. For this reason 10 pixels on the right and 10 pixels on the left for every *z* level has been disregarded in the measurements. If the temperature relative to 20 more external pixels, 10 on the right and 10 on the left, are not, therefore, taken into account, the temperature can be considered constant for each z level, with an error lower than 5 % with respect to the mean value.

In this way a temperature profile of 14 points in z-direction has been obtained every 0.03 s. In order to chose the best function to fit these 14 points, some considerations on the *T(z,t)* function must be made. In fact, if the heat losses through the PTFE ring are considered negligible, the transient temperature function *T(z,t)* can be obtained by the solution of the following differential equation:

$$\alpha \cdot \frac{\partial^2 T(z,t)}{\partial z^2} = \frac{\partial T(z,t)}{\partial t}, \tag{6}$$

with the boundary conditions:

$$\left.\frac{\partial T(z,t)}{\partial z}\right|_{z=0} = \dot{Q}_e / S_e = q_e, \tag{7}$$

$$\left.\frac{\partial T(z,t)}{\partial z}\right|_{z=\sum_{i=1}^{10} L_i} = \dot{Q}_d / S_d = h(t)\left[T\left(\sum_{i=1}^{10} L_i, t\right) - T_S\right]. \tag{8}$$

The shape of the function *T(z,t)* which solves eq.(6) with the boundary conditions expressed in eq.(7) and eq.(8) is unknown, because the heat transfer function *h(t)* in eq.(8) is unknown. The simplest hypothesis is that this function is a line. This assumption is surely wrong, but it may offer the best way of reducing the fitting errors on these few data (only 14). The approximation of this function to a line implies considering the right-hand term of eq.(6) negligible; this is true if the difference in temperature of each point in two consecutive time increments can be considered negligible. In this way, if the time of measurement is sufficiently small, the difference in temperature will be lower than the thermal resolution of the infrared thermo-camera. The maximum rate of change in the temperature of each point must, therefore, be lower than 5 K/s (product of spatial resolution and frequency of measurement), to ensure that this method introduces errors lower than the accuracy of the thermo-camera. The highest temporal temperature gradient in the dissipator is certainly close to the surface wetted by the fluid, because the heat transfer coefficient changes over time. The highest temperature $T_W$, measured close to the surface with a frequency of 0.33 Hz, changes 3.4 K/s. With this method, therefore, the output power $\dot{Q}_d$ is determined by the following equation:

$$\dot{Q}_d(t) = -k \cdot S \cdot \left.\frac{\partial T(z,t)}{\partial z}\right|_{z=L} \cong -k \cdot S \cdot m, \tag{9}$$

where $k$ is the thermal conductivity and $m$ is the angular coefficient of the line equation determined in a least-square sense. A typical evolution of the temperature in the $z$-direction, which has been measured by the thermo-camera every 0.03 s, is shown in Fig. 9. Each point, relative to a level $z$, is the average of the temperature measured in 43 pixels ($x$-direction). These mean temperatures refer to the experimental test carried out with $\dot{Q}_e$ =30 W and $V_T$ =25·10$^{-6}$ m$^3$ at t=200 s, the time when the heating surface could be dry. Even in this case, where the temperature oscillations in time are higher, the linear regression allows an error lower than 0.5%.

Fig. 10 shows the evolutions of $\dot{Q}_d$ in the period t=200-280 s. $\dot{Q}_d$ is calculated with Method A, with Method B or by considering the whole dissipator at the same temperature $T_W$ measured by a thermocouple every 3 s. This figure also shows the input power $\dot{Q}_e$ and the $T_W$ temperature evolution experimentally measured.

Fig. 10 shows that, as soon as the evaporator empties, $\dot{Q}_d$ suddenly falls. In particular, in 4 seconds it falls to 66% of $\dot{Q}_e$. On the other hand. as soon as the valves are opened, $\dot{Q}_d$ suddenly rises and becomes 130% of $\dot{Q}_e$ in 15-20 seconds, because the cold liquid coming from the evaporator removes a power higher than $\dot{Q}_e$ from the dissipater.

Moreover, Fig. 10 shows good agreement between the data calculated with Method A and those measured with Method B. The heat transfer coefficients calculated with Method A are, therefore, confirmed by the measurements of Method B.

## CONCLUSIONS

In the case of indirect cooling, the metallic mass of the evaporator can play an important role in all the periodic cooling devices. This paper presents two different methods of measuring a heat transfer coefficient changing over time. The first achieves this by measuring the temperature close to the heat transfer surface and approximating the temperature distribution in the copper dissipator with a finite difference method, while the second directly measures the output power removed by the cooling fluid. These two methods have shown good agreement if applied to a PTPT device with a periodic heat transfer coefficient. These methods allow the heat transfer coefficient to be measured as the starting volume of the liquid pool decreases in the evaporator down to $3.5\cdot10^{-6}$ m$^3$. In the case of large volumes (>$64\cdot10^{-6}$ m$^3$), the maximum heat transfer coefficient is about 11000 W/m$^2$·K, while for volumes lower than $3.5\cdot10^{-6}$ m$^3$ the maximum heat transfer coefficient is approximately 5000 W/m$^2$·K. The minimum heat transfer coefficient is similar for all volumes and it is about 1100 W/m$^2$·K. As a result, the heat transfer coefficient decreases down to 20% of the maximum for small liquid pool volumes (<$3\cdot10^{-6}$ m$^3$) or down to 9% for large liquid pool volumes (>$64\cdot10^{-6}$ m$^3$).

The heat transfer function has, therefore, been measured accurately, but no quantitative explanation has been given to justify the fall in the heat transfer coefficient of about 50% if the liquid pool volume decreases from 64 to $3.5\cdot10^{-6}$ m$^3$. An experimental study on boiling heat transfers with small pool liquid volumes is currently being carried out by the present authors.

## Nomenclature

*Latin symbols*

| | | |
|---|---|---|
| c | specific heat of the dissipator | [J·kg$^{-1}$] |
| D | diameter | [m] |
| h | heat transfer coefficient | [W·m$^{-2}$·K$^{-1}$] |
| k | thermal conductivity | [W·m$^{-1}$·K$^{-1}$] |
| L | height of a node | [m] |
| m | angular coefficient eq.(9) | [K·W$^{-1}$] |
| M | mass | [kg] |
| q | heat flux | [W·m$^{-2}$] |
| $\dot{Q}$ | thermal power | [W] |
| r | radial coordinate | [m] |
| R | thermal resistance | [K·W$^{-1}$] |
| S | heating surface | [m$^2$] |
| t | time | [s] |
| T | temperature | [K] |
| V | working fluid volume | [m$^3$] |
| x | coordinate | [m] |
| z | coordinate | [m] |

*Greek symbols*

| | | |
|---|---|---|
| $\theta$ | angolar coordinate | [rad] |
| ε | emittance | [dimensionless] |
| α | thermal diffusivity | [m$^2$·s] |

*Subscripts*

| | |
|---|---|
| 1 | OFF time for electrovalves |
| 2 | ON time for electrovalves |
| a | stored heat in the dissipator |
| c | cold source |
| d | dissipating surface |
| e | evaporator |
| e,l | liquid in evaporator |
| env | environment |
| i | node |
| m | intermediate source |
| n | time increment |
| S | saturation condition |
| T | transferred every cycle |
| W | wall |

## References


1. McDonald T.W., Hwang K.S., Diciccio R. Thermosyphon loop performance characteristics. Part 1 Experimental study, *ASHRAE Trans*. 83. Part II, No. 2467. 1997.
2. Ramaswamy C., Joshi Y., Nakayama W., Johnson W. Performance of a compact two-chamber two-phase thermosyphon: effect of evaporator inclination, liquid fill volume and contact resistance, *Proc. Int. Heat Transfer Conf.*, S. Korea, 1998.
3. Min-Kyun Na, Jin-Seok Jeon, Ho-Young Kwak, Sang-Sig Nam, Analytical and experimental studies on a closed loop two-phase thermosyphon for cooling MCM, *Celata, Di Marco, Shah (Eds.), Two-phase Modelling an Experimentation*, Pisa (Italy), 1999. Pp. 553–560.
4. Rhi S.H., Lee Y. Two-phase loop thermosyphons for cooling of electronic system, *Celata, Di Marco, Shah (Eds.), Two-phase Modelling an Experimentation*, Pisa (Italy), 1999. Pp. 561–568.
5. Yuan L., Joshi Y., and Nakayama W. Effect of condenser location and tubing length on the performance of a compact two-phase thermosyphon. Proc. 2001 Int. Mech. Eng. Congress Expo., New York, NY, Nov. 11–16, 2001.
6. Krustalev D. Loop Thermosyphons for Cooling of Electronics, *18th IEEE SEMI-THERM Symposium*, 2002.

7. Pal A., Joshi Y. K., Beitelmal M. H., Patel C. D., Wenger T. M. Design and Performance Evaluation of a Compact Thermosyphon, *IEEE TRANS. on components and packaging technologies.* Vol. 25. 4. 2002.
8. Mukherjee S. and Mudawar I. Smart Pumpless Loop for Micro-Channel Electronic Cooling Using Flat and Enhanced Surfaces, *IEEE TRANS. components and packaging technologies.* Vol. 26. 1. 2003.
9. Khodabandeh R. Thermal performance of a closed advanced two-phase thermosyphon loop for cooling of radio base stations at different operating conditions, *Applied Thermal Engineer*ing 24, 2004.
10. Fantozzi F., Filippeschi S., Latrofa E. Upward and downward heat and mass transfer with miniature periodically operating loop thermosyphons, *Superlattices and Microstructure*, 35 (2004).
11. Fantozzi F., Filippeschi S., Latrofa E. Miniature Pulsated loop thermosyphon for desktop computer cooling: feasibility study and first experimental tests, *5th Minsk Seminar on Heat Pipes, Heat Pumps, Refrigerators*, Minsk, Belarus, 2003.
12. Filippeschi S., Latrofa E., Salvadori G. On the possibility of evaporator drastic scale reduction in a periodically operating two-phase thermosyphon, *Proc. 3rd Int. Symp. on Two-Phase flow modelling and experimentation*, Pisa, Italy, September 22-25, 2004.
13. Fantozzi F., Filippeschi S. Pulsated two-phase thermosyphons for electronic equipment thermal control, *ICES 2002*, San Antonio, Texas, 2002.
14. Fantozzi F., Filippeschi S., Sasin V.J., Savchenkova N.M. Heat transport device based on pulsing thermosyphons with forced fluctuations of pressure, *12 Int. Heat Pipe Conf.*, Moscow, 2002.
15. Lienhard J.H. A Heat Transfer Textbook, *Prentice-Hall: Englewood Cliffs*, New Jersey,1981.
16. Cebeci T. Laminar free convective heat transfer from the outer surface of a vertical slender circular cylinder, *Proc. Fifth Int. Heat Transfer Conf.*, Tokyo, 1981.
17. Guglielmini G., Misale M., Schenone C. Boiling of saturated FC-72 on square pin fin arrays, *Int. J. of Thermal Science* 41, Elsevier Science, 2002.
18. Rainey K. N. et al. Effect of pressure, subcooling, and dissolved gas on pool boiling heat transfer from microporous, square pin-finned surfaces in FC-72, *Int. J. of Heat and Mass Transfer*. Vol. 46. Pp. 23-35, 2003.

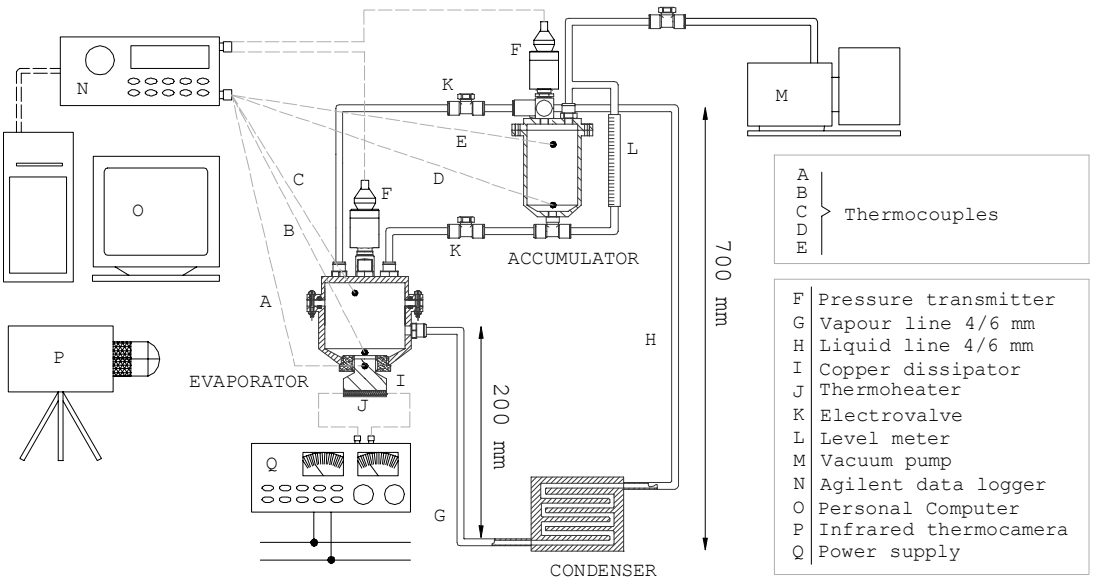


Fig. 1. Experimental facility

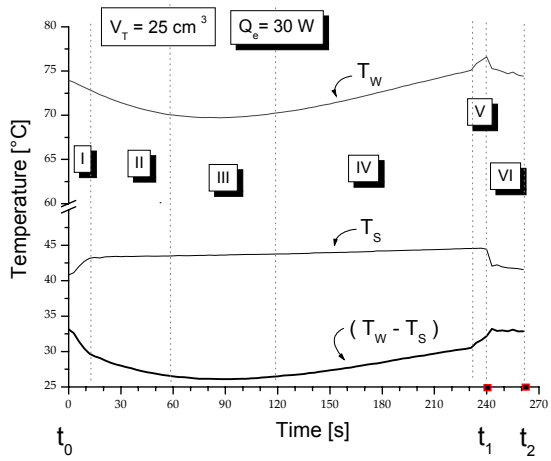


Fig. 2. Evolutions of the temperatures $T_W$ and $T_S$ and the wall superheat ($T_W$-$T_S$) for $\dot{Q}_e$ = 30 W

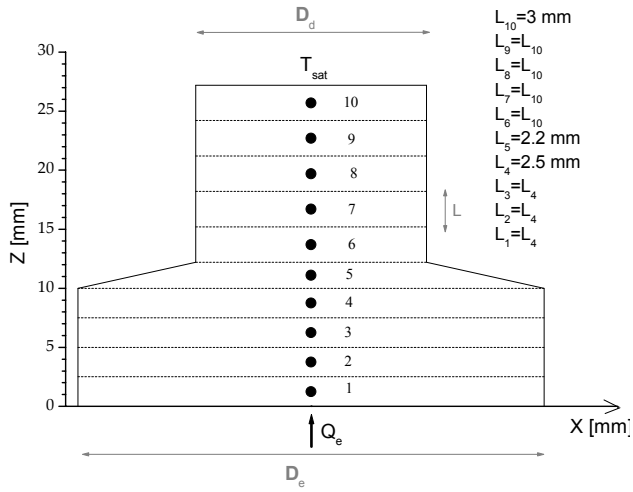


Fig. 3. Finite-difference approximation of the copper dissipator

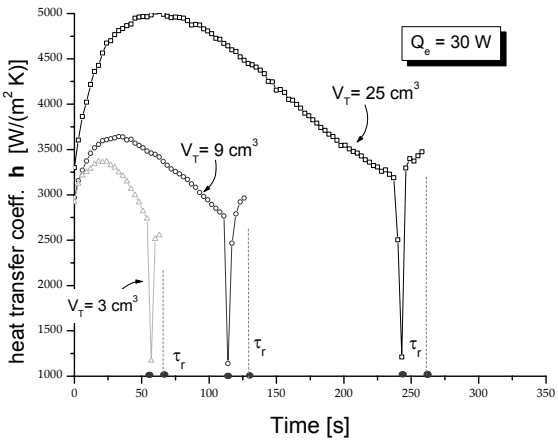


Fig. 4. Evolution of heat transfer coefficient $h$ for $\dot{Q}_e$=30 W ($q_e$=10.83·10$^4$ W·m$^2$, different $V_T$)

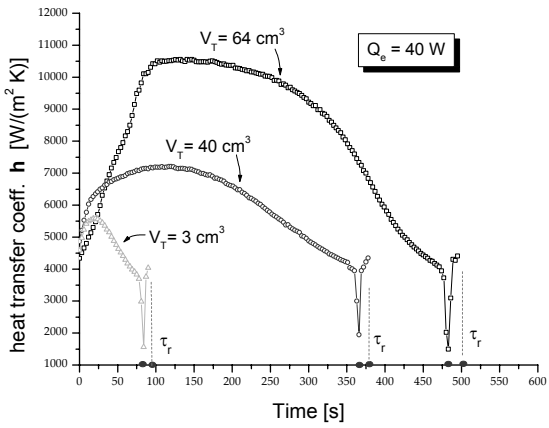


Fig. 5 Evolutions of heat transfer coefficient $h$ for $\dot{Q}_e$=40 W ($q_e$=14.44·10$^4$ W·m$^2$, different $V_T$)

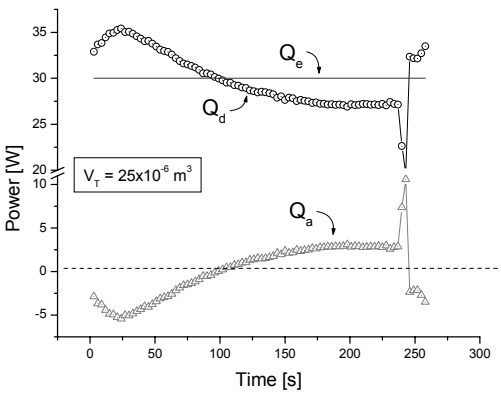


Fig. 6. Evolutions of the power $\dot{Q}_e$, $\dot{Q}_d$, $\dot{Q}_a$ in a single stable periodic regime

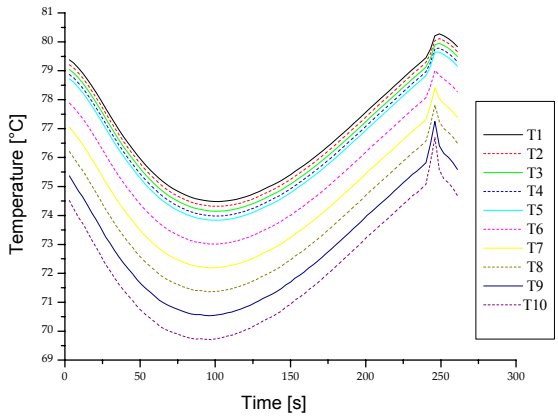


Fig. 7. Evolutions of the $T_i$ (1<i<10) for $\dot{Q}_e$=30 W, $V_T$=25·10$^{-6}$ m$^3$

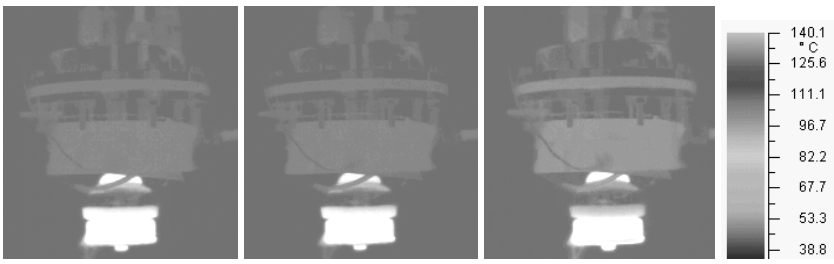


t= 0 s t = 90 s t = 240 s

Fig. 8. Infrared images of the evaporator at different time $q_d$=10.83·10$^4$ W·m$^2$ e $V_T$ = 25·10$^{-6}$ m$^3$

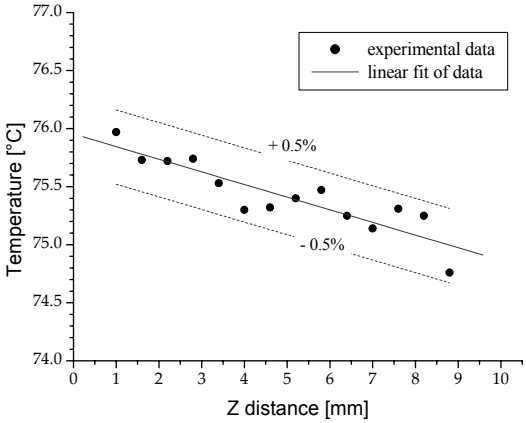


Fig. 9. Mean temperature at different z ($\dot{Q}_e$=30 W, $V_T$=25·10$^{-6}$ m$^3$, $t$=200 s)

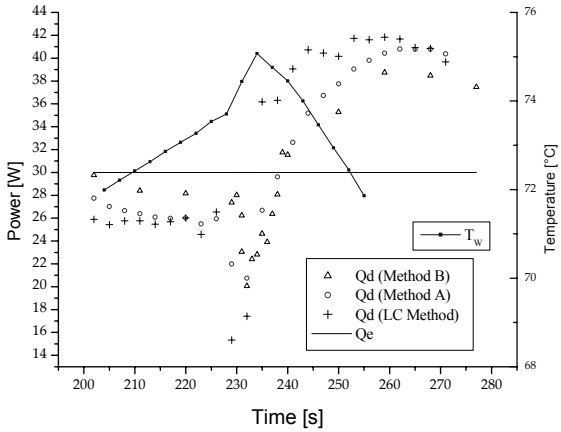


Fig. 10. Dissipated power: comparison of different evaluation methods